Examination of DFT and TDDFT Methods II

Yi-Gui Wang*

Department of Chemistry, Yale University, New Haven, Connecticut 06520-8107

Received: August 11, 2009

We investigated the isomerization energies for C_8 alkanes (*n*-octane and 2,2,3,3-tetra-methyl butane) and 1-X-propenes (X = CH_3, F, Cl, Br) and the excited states for tropolone. The recently implemented TDDFT gradients enabled us to optimize the adiabatic excited-state structures and to obtain wave function files for excited-state electron density analyses with 25 functionals. The dispersion interactions had been found to be important for predicting the isomerization energies for *n*-octane and 2,2,3,3-tetra-methyl butane and for *cis*- and *trans*-1-X-propenes (X = CH_3, F, Cl, Br). B3LYP failed to predict the isomerization energies for the first case but succeeded for the latter. We noticed that the integrated electron density and the merging contour values in the electron density difference plots were related to the isomerization energies; the DFT functionals (LSDA, BHandH, VSXC, and M052X) that could correctly account for the dispersion forces produced a greater electron density response for 2,2,3,3-tetramethyl butane than *n*-octane. Although the faster proton transfer reaction rate in the $\tilde{A}^1B_2$ excited state relative to the $\tilde{X}^1A_1$ ground state of tropolone could be reproduced only by M052X, the three newly designed functionals (BMK, CAM-B3LYP, and M052X) apparently performed better than other DFT functionals. The C−C′ bond lengths of the C_s symmetry excited state were possibly underestimated by DFT methods; the underestimation of C−C′ bond lengths contributed to the high proton transfer barriers in the $\tilde{A}^1B_2$ excited state of tropolone.

1. Introduction

Density functional theory (DFT) was introduced by Kohn and Hohenberg in the 1960s[1,2] and provides a means to approximate electron correlation with resource efficiency similar to that of Hartree−Fock (HF). In the formal DFT theory, the correlation effect is included in the exchange-correlation potential[1−10]

$$v_{xc}(\mathbf{r}) = \frac{\delta E_{xc}[\rho]}{\delta \rho(\mathbf{r})} \quad (1)$$

The exact formula of $v_{xc}(\mathbf{r})$ is unknown, and the practical implementation approximates $v_{xc}(\mathbf{r})$ by different approaches.

The local spin density approximation (LSDA)[11] has been widely used in physics for decades, whereas the extensive applications of DFT methods in chemistry did not commence until the hybrid B3LYP functional was introduced by Becke in 1993.[12a] In the past decade, B3LYP has largely replaced MP2 in theoretical energy evaluations. However, B3LYP has recently been found to be unable to predict the correct isomerization energy for simple alkanes, and the error increases along with the size of the alkane systems.[13−15] For example, B3LYP produces an error as large as 11 kcal/mol for C_8 alkanes (i.e., *n*-octane and 2,2,3,3-tetramethylbutane). In the meantime, a large number of new DFT functionals have been proposed. What functionals should be used when the B3LYP functional fails?

Although the energetic is important in many fields such as drug discovery and others, the geometrical optimization is pivotal in chemistry. To carry out geometrical optimization effectively, the technique of energy gradient should be developed for DFT and TDDFT methods. Moreover, the technique of energy gradient enables us to write out wave function files, which are the basis of our theoretical density analysis. For the excited states, Van Caillie and Amos worked out the gradient of energy at the TD-LDA level almost 10 years ago,[16] and Furche and Ahlrichs also implemented this technique later.[17] Scalmani et al. extended this technique to include the solvent effects within the polarized continuum model (PCM) and made it available for all new functionals in Gaussian program packages.[18]

In this article, we reviewed the dispersion problem and new DFT functionals in Section 2. Then, the isomerization energies of the C_8 alkanes (Section 3) and of the cis and trans isomers of 1-X-propenes (X = F, Cl, Br, CH_3) (Section 5) were calculated with 25 DFT functionals and compared with the HF and the CCSD results to conclude that the "error cancellation" was related to the response of density. At last, the proton transfer reactions in the $\tilde{X}^1A_1$and the $\tilde{A}^1B_2$ states of tropolone were investigated to demonstrate that the availability of a large number of DFT functionals for general users provided a unique way to deal with new chemical problems.

2. Dispersion Problem and New Density Functional Theory Functionals

Grimme et al. studied alkanes and other systems carefully. First, they suggested to avoid hybrid functionals entirely;[13b] then, they attributed this DFT caveat to the improper treatment of medium range correlation.[13a] Lastly, they concluded that the lack of dispersion was the dominant factor.[13c] Including the empirical dispersion term in B3LYP, Schwabe and Grimme successfully reduced the maximum absolute errors (MAEs) from 5.6 to 3.1 kcal/mol for the full G3/99 set of 223 samples of heats of formation.[13c] Other studies indicated that the inclusion of dispersion interactions would not be sufficient to alleviate the DFT deficiencies.[14] In a recent and more extensive study on 622 neutral closed-shell organic compounds, Tirado-Rives and Jorgensen reported that the inclusion of the dispersion correction

* Corresponding author.

10.1021/jp9077739 CCC: $40.75
Published on Web 09/16/2009

TABLE 1: Isomerization Energy and Enthalpy from *n*-Octane → 2,2,3,3-Tetramethylbutane (kilocalories per mole)

	ΔE^a aug-cc-pVDZ	aug-cc-pVTZ	ΔE^b aug-cc-pVDZ	$\Delta H(0K)^c$ aug-cc-pVDZ	$\Delta H^0(298K)^d$ aug-cc-pVDZ
HF	10.58	11.48	10.84	9.92	8.95
B3LYP	6.58	7.92	6.70	5.71	4.91
M052X	−2.20	−0.42	−2.33	−3.41	−4.12
MP2	−6.66	−4.61	−6.77	−7.91	−8.74
LSDA	−4.47	−3.06	−5.34	−6.57	−7.33
CCSD			−2.23		
exptl	-1.9 ± 0.5[35a]				-4.05 ± 0.71[65]

[a] B3LYP/aug-cc-pVDZ structure. [b] MP2/6-311+G(d,p) structure. [c] Structures are fully optimized at the corresponding levels. ΔH^0 is standard enthalpy at 298 K. [d] Structures are fully optimized at the corresponding levels. ΔH^0 is standard enthalpy at 298 K.

in B3LYP could significantly reduce the MAE bar; nonetheless, 2.0 kcal/mol seems to be an accuracy limit in predicting isomerization energies and heats of formation.[15]

The DFT methods have some well-known challenges: (1) the electron density is a short-range (local) property, and (2) unlike HF, DFT methods have self interaction, particularly for the one-electron system like the proton.[3,19] HF exchange has been included in hybrid functionals to compensate for DFT shortcomings. First, HF has a long-range property, and second, HF does not suffer from a self-interaction problem. The half-and-half functional (BHandHlyp) mixes the HF and DFT exchange contributions in a 1:1 ratio, and the 50% exchange underlines the impact of the HF exchange.[20] Also, on the basis of B3LYP, two popular functionals are proposed to improve the DFT functional exchange potential. One such functional is OPTX, which includes not only exchange but also left−right correlation;[21] the other approach is to adopt Gaussian-like behavior at long-range for an exact exchange energy density.[22] The latter approach is designed to treat biological systems (H-bonding) accurately. The resultant functionals are two B3LYP variants: O3LYP and X3LYP. In recent years, great efforts have been made to obtain optimum generalized gradient approximation (GGA) functionals to tackle the local limitation of DFT methods. Two representative functionals in this regard are PBEPBE[23] and THCTH.[24] The PBE exchange is a simplified GGA functional in which all of the parameters are fundamental constants (i.e., no empirical parameters), whereas HCTH is a heavily parametrized functional that contains 15 adjustable parameters. Early studies have shown that the accuracy of reaction barrier heights can be dramatically improved by increasing the percentage of "exact" exchange into the 40−50% region, but the performance for other properties is seriously degraded.[25−27] Including the kinetic energy density was found to correct "back" excess exchange mixing for the ground states (i.e., balanced description); BMK, possessing 42% exact exchange, was designed with this consideration in mind to make headway toward developing all-purpose functionals.[28] Although DFT is formally a ground-state theory, a time-dependent procedure (TDDFT) can be used to study excited states.[29−38] Because long-range properties, such as charge transfer, are common in the excited states, DFT methods might encounter severe problems for the excited states.[32] A new functional, Coulomb-attenuating method-B3LYP (CAM-B3LYP), takes into long-range interactions by comprising 0.19 HF and 0.81 B88 exchange at short-range and 0.65 HF plus 0.35 B88 at long-range.[39] Recent studies clearly demonstrate that the CAM-B3LYP functional successfully handled charge transfer.[40] Besides considering well-known strategies, empirical fit was employed to calibrate newly designed functionals. Several sets of carefully selected databases are used to refine parameters of new functionals quantitatively. The database sets include thermochemistry, diverse barrier heights, noncovalent interaction energies, and transition-metal reaction energies. M052X is one such functional.[41] In the case of the isomerization energy of C_8 alkanes, the success of M052X has been evaluated by its designers Zhao and Truhlar and was attributed to the most attractive correlation of M052X in the medium range (3−5 Å) among forty tested functionals.[42]

We classified all 24 DFT functionals (excluding LSDA) into three categories: pure GGA functionals (BLYP,[43,44] OLYP,[21,44] BP86,[43,45] PBEPBE,[23] HCTH[24]), pure τ functionals (THCTH,[46] BB95,[43,47] VSXC,[48a] TPSSTPSS[49]), and hybrid functionals (M05,[50] M052X,[41] O3LYP,[21,44] X3LYP,[22a] B3LYP,[12,44] B3P86,[12a,45] PBE1PBE,[51] B1B95,[43,47] THCTHHYB,[46] TPSSH,[52] BMK,[28] BHandH,[43,44] BHandHHYB,[20,43,44] HSE2PBE,[23,53] HSE1PBE,[23,53] CAM-B3LYP[39]).

3. Isomerization Energy for *n*-Octane and 2,2,3,3-Tetramethylbutane

The available experimental data for the isomerization standard enthalpy from *n*-octane to 2,2,3,3-tetramethylbutane was −4.05 kcal/mol. This standard enthalpy was derived from the measurement of standard enthalpy of combustion for liquid *n*-octane and crystalline 2,2,3,3-tetramethylbutane.[54] To compare with calculated results, we need to know the zero-point energy contribution and isomer population contribution. It is clear that 2,2,3,3-tetramethylbutane has only one global energy minimum, and *n*-octane may possess many local minima due to the flexibility of the carbon chain. The all-trans conformer is the global minimum for *n*-octane, which was confirmed by calculations at both MP2/6-311+G(d,p) and B3LYP/aug-cc-pVDZ levels. An extensive study for *n*-alkanes in both gas phase and pure liquids found that the all-trans conformer would be the global minimum until $n = 16-18$.[55] For *n*-octane, we performed a Monte Carlo (MC) conformer search with OPLS-AA force field[56] and located 17 more conformers that were 1.0−6.7 kcal/mol higher in total electronic energy than the all-trans conformer. The relative energies of conformers were used to estimate the conformer population. With zero-point energy and conformer population corrections, the ΔH (298K) between all-trans *n*-octane and 2,2,3,3-tetramethylbutane should be ∼−4.45 kcal/mol at the M052X/aug-cc-pVDZ level, agreeing with the experimental standard enthalpy of -4.05 ± 0.71 kcal/mol.[55] At the M052X/aug-cc-pVDZ level, the relative total energy was ∼−2.20 kcal/mol (Table 1), agreeing remarkably well with CCSD results and in turn according well with previously estimated ΔE value of -1.9 ± 0.5 kcal/mol.[13a]

The standard calculation levels had modest effects on the results. We optimized structures of two isomers at two different levels: MP2/6-311+G(d,p) and B3LYP/aug-cc-pVDZ. The MP2/6-311+G(d,p) level predicted slightly shorter C−C bonds than those at the B3LYP/aug-cc-pVDZ level (by 0.003 Å in

chain structure, by 0.007 Å for terminal C−C, and by 0.018 Å for central C−C in branch structure). Except for LSDA, two sets of structures gave similar ΔE, and the bigger basis set aug-cc-pVTZ was generally in favor of the all-trans chain structure by 1 to 2 kcal/mol (cf. Table 1). Nonetheless, the overall trend was obvious: HF and B3LYP results had incorrect signs, but M052X along with MP2 and CCSD correctly showed the relative stability of two isomers. Among all 25 tested functionals at the DFT/aug-cc-pVDZ level (Table S1 in the Supporting Information), only four predicted the correct sign (LSDA, BHandH, VSXC, and M052X). Of note, the success of LSDA and BHandH predicting isomerization energies came as a surprise; also, VSXC overestimated the stability of 2,2,3,3-tetra-methyl butane by a large margin (−24.08 kcal/mol).

Interestingly, the success of LSDA and BHandH and the failure of B3LYP were not due to the correlation effects but rather due to the density distribution. Despite the fact that LSDA and BHandH are the only two functionals that predict higher total energies than all other DFT methods and than the correlated conventional methods (MP2 and CCSD) (Table S1 in the Supporting Information), they provide more density between terminal groups than B3LYP does. In MP2-HF electron density difference plots, the positive contours merged with adjacent carbons for both 2,2,3,3-tetra-methyl butane and *n*-octane. This density cloud was assumed to provide stabilization energy that is missing in the HF method. Because there are more 1,4 C,C interactions for 2,2,3,3-tetra-methyl butane than for *n*-octane, 2,2,3,3-tetra-methyl butane was lower in electronic energy than *n*-octane. In B3LYP-HF electron density difference plots, electron density increasing regions were still separated and localized around carbons and hydrogens, so B3LYP gave the wrong sign of isomerization energy. The LSDA-HF electron density difference plots demonstrated the merging electron density cloud around adjacent carbons, and LSDA predicted the correct sign of isomerization energy.

The integrated electron density and the merging electron density contour values gave us more insights. The integrated density is the electron density enclosed within the depletion and increasing regions in the density difference plots. The merging contour values are the minimal electron density contour values, at which electron density from two separated methyl groups start to join each other (Figure 1). (1) The CCSD method gave the best isomerization energy (Table 2), and we noticed that CCSD was adequately in favor of 2,2,3,3-tetra-methyl butane over the all-trans isoformer; the integrated density is 0.01e more and the merging contour value is 0.0001 e/a_0^3 larger. 2) The total B3LYP integrated density for *n*-octane was only 0.005e smaller than that for 2,2,3,3-tetra-methyl butane. However, the merging electron density contour of B3LYP electron density was the smallest among all methods (0.0003 e/a_0^3). As a result, B3LYP is only slightly better than HF in predicting the isomerization energy. (3) The merging contour of VSXC electron density was also 0.0003 for *n*-octane, but that for 2,2,3,3-tetra-methyl butane was substantially high (0.00085). In addition, the integrated electron density was much larger (by 0.05e) for 2,2,3,3-tetra-methyl butane than that for *n*-octane. Therefore, VSXC strongly overestimated the isomerization energy. (4) LSDA was designed to be dependent on only α- and β-spin density, so it is the least similar to HF and gives the largest integrated electron density. LSDA had greater integrated electron density difference between two isomers than CCSD, which was consistent with the overestimation of isomerization energy by LSDA. (5) The situation for MP2 was similar to that for LSDA, except MP2 had smaller magnitudes for both integrated density and the merging contour value. (6) Both M052X and BHandH gave reasonable isomerization energies, but the merging contour value of M052X density was 0.0004 in favor of 2,2,3,3-tetra-methyl butane, whereas that of BHandH is only 0.0001. This finding was in accord with the stronger electron correlation potential of M052X in the medium range (3−5 Å).[42]

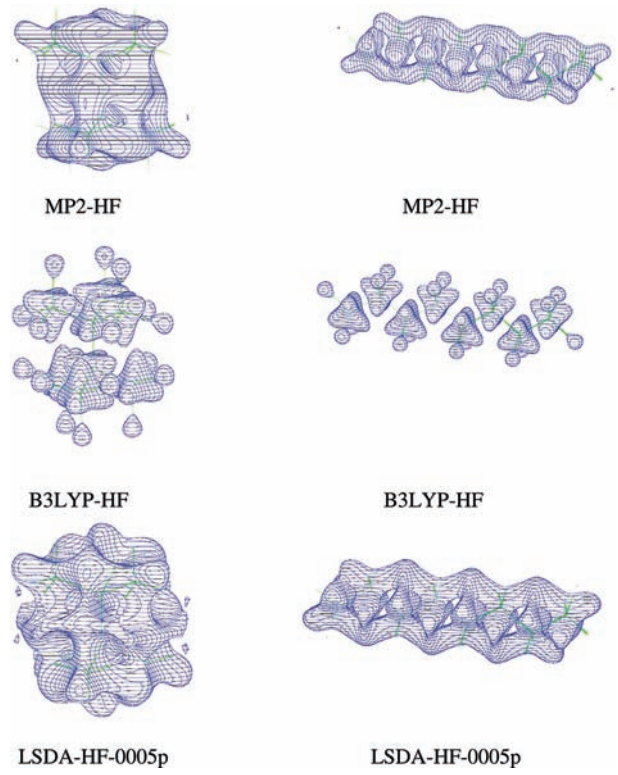

Figure 1. Electron density increasing regions of *n*-octane and 2,2,3,3,-tetra-methyl butane in comparison with HF density (0.0005 au contour).

TABLE 2: Magnitude of Integrated Electron Density (*e*) for Electron Density Difference Plots, Merging Contour Values (au Data in Brackets), and Isomerization Energy (kilocalories per mole)

	chain	branch	isomerization energy
MP2-HF	0.4672(0.0008)	0.4925(0.00095)	−6.77
B3LYP-HF	0.5720(0.0002)	0.5771(0.0003)	6.70
M052X-HF	0.5412(0.0008)	0.5559(0.0012)	−2.33
VSXC-HF	0.5220(0.0003)	0.5772(0.00085)	−27.13
LSDA-HF	0.8981(0.0011)	0.9268(0.0013)	−5.34
BHandH-HF	0.5809(0.0008)	0.5912(0.0009)	−3.04
CCSD-HF	0.3724(0.00045)	0.3857(0.00055)	−2.23

4. 1-X-Propenes (X = CH_3, F, Cl, Br)

A very recent study indicated that all three types of intramolecular interactions (electronic static, steric, and dispersion) were significant in determining the cis/trans relative energies for 1-X-propenes (X = CH_3, F, Cl, Br).[57] This detailed study provided a valuable basis to assess the DFT methods. We used the CCSD/6-311++G** optimized structures and aug-cc-pVTZ basis sets to calculate energies with HF, MP2, CCSD, and 25 DFT functionals (Figure 2 and Table S2 in the Supporting Information). 1-X-propenes are ideal compounds for studying the interactions between terminal groups because all bonds are the same for two isomers, and the double bond constrains the molecule to remain in one plane.

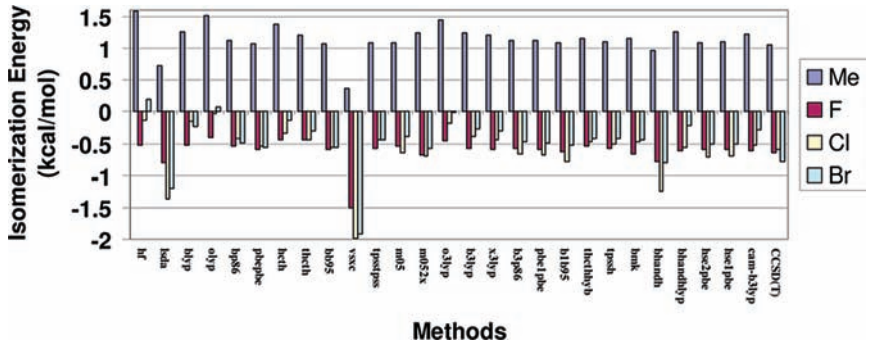

Figure 2. Isomerization energies (kilocalories per mole) for 1-substituted propenes. (The methods are HF, LSDA, BLYP, OLYP, BP86, PBEPBE, HCTH, THCTH, BB95, VSXC, TPSSTPSS, M05, M052X, O3LYP, B3LYP, X3LYP, B3P86, PBE1PBE, B1B95, THCTHHYB, HSE2PBE, HSE1PBE, CAM-B3LYP, and CCSD(T) from left to right).

Despite the fact that the dispersion interactions were also important for the isomerization energies of *cis*-/*trans*-1-X-propenes, almost all DFT functionals correctly recovered the small energy preference for cis isomers (X = F, Cl, Br) or for the trans isomer (X = Me) (Figure 2 and Table S2 in the Supporting Information). The B3LYP isomerization energies were reasonably similar to CCSD(T) isomerization energies. The B3LYP isomerization energies were decreasing in the order of F, Cl, and Br, whereas CCSD(T) isomerization energies were roughly the same for these three pairs of 1-substituted propenes. Therefore, the B3LYP method underestimated the isomerization energy by 0.5 kcal/mol for 1-Br-propenes (Table S2 in the Supporting Information). The B3LYP method could also reproduce the sign of isomerization energies with different C═C bond lengths. For 1-chloro-propene, we arbitrarily constrained the central C═C bond lengths to 1.2, 1.33, and 1.8 Å and compared the isomerization energies. The relative energies between cis and trans isomers were 0.25, −0.40, and −0.91 kcal/mol at B3LYP/6-311++G(2df,2p) level and 0.09, −0.47, and −0.80 kcal/mol at the CCSD/6-311++G(2df,2p) level. The reasonable agreement between B3LYP isomerization energies and CCSD(T) isomerization energies indicated the fact that the special structures of 1-X-propenes could be the reason for alleviating the deficiencies of B3LYP in dealing with dispersion interactions. The double bond of 1-X-propenes contributed to the good performance of B3LYP because the double bonds demonstrated significant correlation effects.[10,42,44,46] VSXC was designed by specifically considering the kinetic-energy-density dependence.[48] LSDA was designed by considering only the energetic dependence of α-spin and β-spin electron density. Both VSXC and LSDA overestimated dispersion interactions, indicating that the dispersion interactions had kinetic nature. Nevertheless, density distribution again played a role here because B3LYP indeed put more density between two terminal groups of cis conformers than CCSD does (Figure S1in the Supporting Information).

5. Proton Transfer Barriers in the $\tilde{X}^1A_1$ and the $\tilde{A}^1B_2$ States of Tropolone

The proton transfer of tropolone is a very complicated reaction and may pose challenges for DFT/TDDFT methods for three separate reasons: (1) the proton in the transition state of the reaction is loosely bound; (2) the proton migration may induce a problem of self interaction; and (3) charge transfer may complicate the situation because a seven-member ring is conjugated to the reaction center. Fortunately, both experimental[58,59] and high-level theoretical studies[60] were available for this reaction. Because of the large size of tropolone, we selected only a set of representative DFT/TDDFT methods and used aug-cc-pVDZ basis sets.

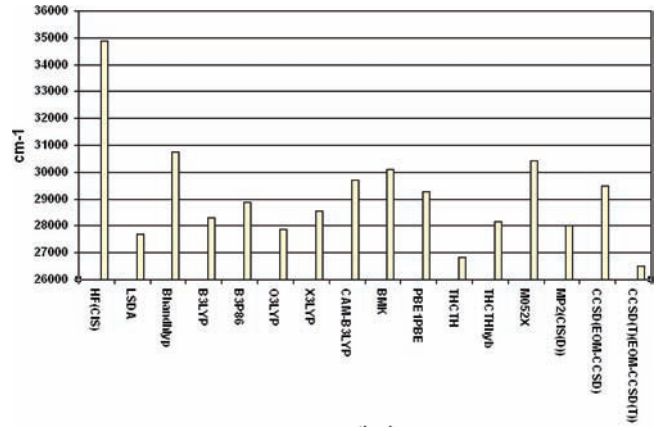

Figure 3. Adiabatic excitation energies for $\tilde{A}^1B_2$ states of planar (Cs) tropolone.

The experimental adiabatic excitation energy of the $\tilde{A}^1B_2$ state of tropolone was 27 017.690 ± 0.012 cm^{-1}.[58,59] CIS significantly overestimated the adiabatic excitation energy (by 7883 cm^{-1}) (Figure 3 and Table S3 in the Supporting Information). All DFT/TDDFT methods reduced the errors to be −205 to 3733 cm^{-1}, and the performance of LSDA (excitation energy was 685 cm^{-1} higher than the experimental value) was remarkable. TDDFT methods (especially B3P86) had been found to predict reasonable vertical excitation energies for carbonyl compounds.[30] Apparently, EOM-CCSD(T) gave an excellent estimation of the vertical excitation energies, only 517 cm^{-1} lower than the experimental value.

Experiments[58,59] established the fact that the proton transfer of tropolone in the $\tilde{A}^1B_2$ state was faster than its proton transfer in the ground state. EOM-CCSD and CIS(D) methods correctly reproduced the lower barrier in the excited state.[60] CIS also demonstrated the fact that the proton transfer reaction was faster in the excited state, although the absolute barriers were too high in both ground states and excited states. However, TDDFT(DFT) methods predicted a slower proton transfer rate (i.e., higher barrier) for the excited states than for the ground states (Figure 4).

Several special conclusions about the performance of TDDFT methods could be drawn from Figure 4: (1) Although LSDA performed remarkably well in predicting the adiabatic excitation energies of tropolone, LSDA failed to predict proton transfer barriers. (2) The injection of HF exchange in B3LYP was not successful in improving the proton transfer barriers. (3) Neither PBE1PBE and THCTH nor O3LYP and X3LYP invoked further

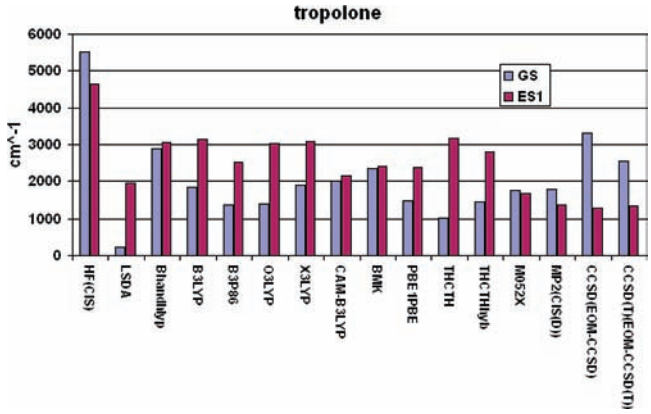

Figure 4. Proton transfer barrier (inverse centimeters) for $\tilde{X}^1A_1$ (GS, ground state) and $\tilde{A}^1B_2$ (ES1 excited state) of tropolone.

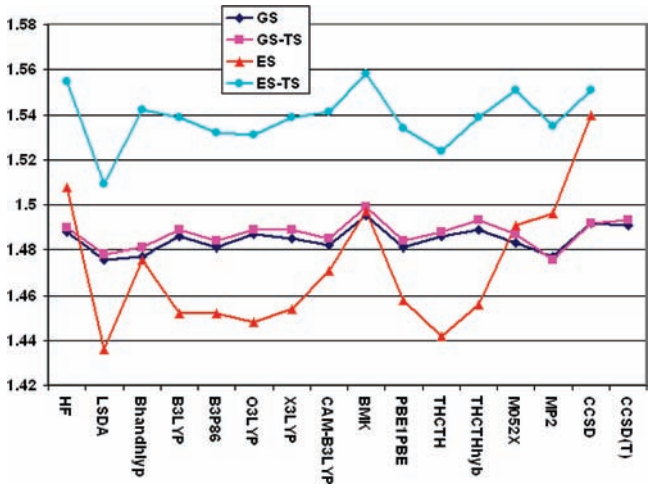

Figure 5. Distance of the bridge C−C′ bond of tropolone. (GS: ground states; ES: excited states; TS: transition states).

improvements over B3LYP. (4) Nevertheless, in the excited state, BHandHlyp brought the proton transfer reaction barriers to be close to that of the ground state, indicating that the large portion of exact HF exchange was important for studying the proton transfer of tropolone. (5) The barrier heights for excited states were close to those of ground states with all three newly developed functionals: BMK, M052X, and CAM-B3LYP. The M052X functional even corrected the trend, although the barrier difference for faster reaction in the excited state was not significant.

The accuracy of barrier heights can be further improved if we consider the optimized structures of tropolone. Figure 5 plotted the bond lengths of bridge C−C′ bond lengths predicted by different DFT functionals. It was evident that the C−C′ bond lengths behaved differently in the $\tilde{X}^1A_1$ and $\tilde{A}^1B_2$ states of tropolone. Both CIS and EOM-CCSD indicated that the C−C′ bond would be longer than 1.5 Å in the excited states, whereas all TDDFT methods gave shorter bridge bond lengths in the C_s symmetry excited states; the exact values varied for different functionals. It is interesting that those functionals having good barrier heights (BHandHlyp, BMK, and M052X) also had long C−C′ bond lengths. Therefore, because the C−C′ bond lengths were close in C_s and C_{2v} symmetry ground states, we recalculated the C_s symmetry excited states using the optimized C−C′ bond length of C_{2v} transition states. Indeed, we successfully reduced the barrier heights of the excited states. For example, the reaction barrier reduced from 3150 to 2605 cm^{-1} at the TD-B3LYP level and from 1656 to 1474 cm^{-1} at the TD-M052X level. One recent CASSCF study gave an optimized C−C′ bond length of 1.41 Å for the excited C_s symmetry tropolone, which was close to our TD-B3LYP result.[61] However, the reaction barrier was either too high (19.33 kcal/mol with CASSCF) or too low (−9.08 kcal/mol with CASPT2).[61] We believe that EOM-CCSD's C−C′ bond length was accurate. Additional support came from comparing results of M052X with B3LYP: (1) the improvement of the M052X reaction barrier coincided with the increased C−C′ bond lengths and (2) M052X has been parametrized to predict the bond length alternation of conjugated chains with great accuracy.[62] Consequently, the conjugated seven-member ring of tropolone should not cause problems for M052X functionals.

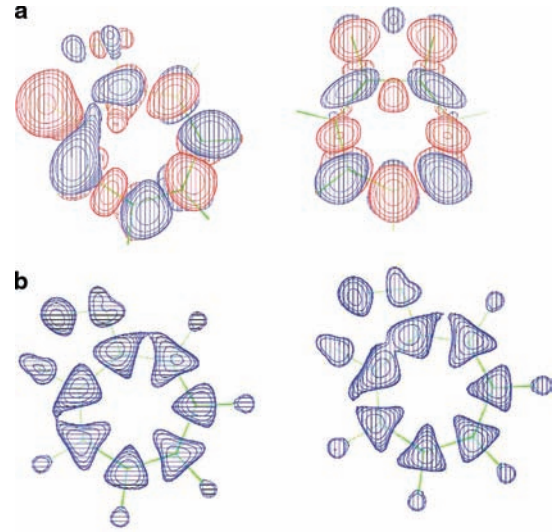

Figure 6. Electron density difference plots for tropolone. (a) Density differences plots for the $\tilde{A}^1B_2$ excited states of tropolone (0.001 e/a_0^3 contour). (b) Electron density increasing regions for C_s symmetry tropolone from CIS(HF) to (TD-)B3LYP (0.002 e/a_0^3 contour).

The characteristics of the $\tilde{A}^1B_2$ excited state of tropolone were depicted by the B3LYP electron density difference plots (Figure 6a). There were electron density increasing regions (blue) between two bridge carbons in the C_s symmetry tropolone, whereas electron density depletion regions (red) could be noticed in the C_{2v} symmetry troplone. These results were in agreement with the shorter C−C′ bond in the excited C_s symmetry tropolone and longer C−C′ bond in the excited C_{2v} symmetry tropolone in comparison with corresponding ground states. More insight can be gained when looking at the density increasing regions from CIS(HF) to TD-B3LYP(B3LYP (Figure 6b). TD-B3LYP apparently had accumulated density in the region of bridge C−C bonds in the excited state, whereas B3LYP put more electron density on two ring C−C bonds. Therefore, the bridge C−C bond was predicted to be much shorter by TD-B3LYP than by CIS.

6. Discussion

During the course of the investigation, we employed several basis sets ranging from 6-311++G** to aug-cc-pVTZ. We made sure that the final conclusions were confirmed at the DFT/aug-cc-pvTZ and CCSD(T)/aug-cc-pVTZ levels. The large basis sets and triples in CCSD(T) had noticeable impact on the calculated values. The B3LYP isomerization energies for C_8 alkanes had an error of ∼11 kcal/mol in other studies[13,14] and had an error of about 9 kcal/mol with aug-cc-pVDZ basis sets.

Better adiabatic excitation energies were also obtained for tropolone with the CCSD(T) method than with the CCSD (Figure 3 and ref 60). The predicted relative energies for *cis*/*trans*-1-X-propenes could be ~0.5 kcal/mol smaller at the B3LYP/aug-cc-pVTZ level than at the CCSD(T)/aug-cc-pVTZ level.[57]

According to the Kohn−Hohenberg theory, the properties are uniquely related to the density. The correct predictions indeed came along with the density consequences in the cases of C_8 alkanes and 1-X-propenes; however, neither the pure GGA functionals nor the pure τ functionals performed significantly better than hybrid functionals in all cases studied here. The pure τ function VSXC is sensitive to the dispersion force, but it normally overestimates this kind of interaction. Because the dispersion forces are of induced-dipole−induced-dipole characteristics, the net change in density might not be significant. The hybrid DFT functionals with large portions of exact exchange are necessary for the study of the excited state of tropolone and the dispersion forces of C_8 alkanes and 1-X-propenes.

7. Conclusions

The faster proton transfer reaction rate in the $\tilde{A}^1B_2$ excited state relative to the $\tilde{X}^1A_1$ground state could be reproduced only by the M052X functional. The newly designed three functionals, BMK, CAM-B3LYP, and M052X, apparently performed better than other DFT functionals. The underestimation of C−C′ bond lengths of C_s symmetry excited states contributed to the high reaction barriers in the excited states of tropolone; the predictions of the proton transfer barriers in the excited states did improve when structures with arbitrarily lengthened C−C′ bond lengths were used. The availability of a large number of DFT functionals for general users provided a unique way to deal with new chemical problems

The electron density difference plots and the merging contour values were directly related to the isomerization energies for *n*-octane and 2,2,3,3-tetra-methyl butane. In the case of C_8 alkanes, B3LYP had an error as large as 9.0 kcal/mol. The DFT functionals that could correctly account for the dispersion forces produced more electron density responses for 2,2,3,3-tetramethyl butane than for *n*-octane. B3LYP performed very well in predicting isomerization energies between *cis*- and *trans*-1-X-propenes (X = CH_3, F, Cl, Br), demonstrating the fact that B3LYP could account for the dispersion energies in the case of 1-X-propenes. The "error cancellation" was related to the response of density.

The hybrid DFT functionals with large portions of exact exchange are necessary for the study of the excited state of tropolone and the dispersion forces of C_8 alkanes and 1-X-propenes.

8. Calculations

The Monte Carlo simulation was carried out with the BOSS program.[63] Both CIS and TDDFT (DFT) calculations were done with a development version of GAUSSIAN;[64] CASGEN[65] was used to make the electron density difference plots.

Acknowledgment. We thank Lori Burns for sharing her EOM-CCSD results of tropolone.

Supporting Information Available: Total energies and isomerization energies of C_8 alkanes, relative energies for cis/trans isomers of 1-X-peopenes (X = CH_3, F, Cl, Br), barriers of the proton transfer reactions in the ground and excited states of tropolone and the adiabatic excitation energies, and electron density difference plots for 1-X-propenes (X = CH_3, F, Cl, Br) between CCSD and B3LYP with 6-311++G(2df,2p) basis sets. This material is available free of charge via the Internet at http://pubs.acs.org.

References and Notes

(1) Hohenberg, P.; Kohn, W. *Phys. Rev.* **1964**, *136*, B864.
(2) Kohn, W.; Sham, L. J. *Phys. Rev.* **1965**, *140*, A1133.
(3) Piela, L. *Ideas of Quantum Chemistry*; Elsevier: Amsterdam, 2007; pp 567−614.
(4) Koch, W.; Holthausen, M. C. *A Chemist's Guide to Density Functional Theory*; Wiley-VCH: Weinheim, Germany, 2000.
(5) Parr, R. G. *Annu. Rev. Phys. Chem.* **1983**, *34*, 631.
(6) Parr, R. G.; Yang, W. *Annu. Rev. Phys. Chem.* **1995**, *46*, 701.
(7) Parr, R. G.; Yang, W. *Density-Functional Theory of Atoms and Molecules*; Oxford University Press: Oxford, U.K., 1989.
(8) Scuseria, G. E.; Staroverov, V. N. In *Theory and Applications of Computational Chemistry: The First Forty Years*; Dykstra, C. E., Frenking, G., Kim, K. S., Scuseria, G. E., Eds.; Elsevier: Amsterdam, 2005; pp 669−724.
(9) Nakano, H.; Nakajima, T.; Tsuneda, T.; Hirao, K. In *Theory and Applications of Computational Chemistry: The First Forty Years*; Dykstra, C. E., Frenking, G., Kim, K. S., Scuseria, G. E., Eds.; Elsevier: Amsterdam, 2005; pp 507−580.
(10) (a) de Proft, F.; Sablon, N.; Tozer, D. J.; Geerlings, P. *Faraday Discuss.* **2007**, *135*, 151. (b) Ayers, P. W. *Faraday Discuss.* **2007**, *135*, 161. (c) Chandra, A. K.; Nguyen, M. T. *Faraday Discuss.* **2007**, *135*, 191. (d) Glukhov, I. V.; Lyssenko, K. A.; Korlyukov, A. A.; Antipin, Y. M. *Faraday Discuss.* **2007**, *135*, 203. (e) Garcia, P.; Dahaoui, S.; Katan, C.; Souhassou, M.; Lecomte, C. *Faraday Discuss.* **2007**, *135*, 217. (f) Bader, R. F. W.; et al. *Faraday Discuss.* **2007**, *135*, 237.
(11) (a) Slater, J. C. *Quantum Theory of Molecular and Solids: The Self-Consistent Field for Molecular and Solids*; McGraw-Hill: New York, 1974; Vol. 4. (b) Vosko, S. H.; Wilk, L.; Nusair, M. *Can. J. Phys.* **1980**, *58*, 1200.
(12) (a) Becke, A. D. *J. Chem. Phys.* **1993**, *98*, 5648. (b) Stephens, P. J.; Devlin, F. J.; Chabalowski, C. F.; Frisch, M. J. *J. Phys. Chem.* **1994**, *98*, 11623.
(13) (a) Grimme, S. *Angew. Chem., Int. Ed.* **2006**, *45*, 4460. (b) Grimme, S.; Steinmetz, M.; Korth, M. *J. Org. Chem.* **2007**, *72*, 2118. (c) Schwabe, T.; Grimme, S. *Phys. Chem. Chem. Phys.* **2007**, *9*, 3397.
(14) Schreiner, P. R. *Angew. Chem., Int. Ed.* **2007**, *46*, 4217.
(15) Tirado-Rives, J.; Jorgensen, W. L. *J. Chem. Theory Comput.* **2008**, *4*, 297.
(16) (a) Van Caillie, C.; Amos, R. D. *Chem. Phys. Lett.* **2000**, *317*, 159. (b) Van Caillie, C.; Amos, R. D. *Chem. Phys. Lett.* **1999**, *308*, 249.
(17) Furche, F.; Ahlrichs, R. A. *J. Chem. Phys.* **2002**, *117*, 7433.
(18) Scalmani, G.; Frisch, M. J.; Mennucci, B.; Tomasi, J.; Cammi, R.; Barone, V. *J. Chem. Phys.* **2006**, *124*, 094107.
(19) (a) Polo, V.; Gräfenstein, J.; Kraka, E.; Cremer, D. *Theor. Chem. Acc.* **2003**, *109*, 22. (b) Gräfenstein, J.; Kraka, E.; Cremer, D. *J. Chem. Phys.* **2004**, *120*, 524.
(20) Becke, A. D. *J. Chem. Phys.* **1993**, *98*, 1372. The defined BHandHlyp in the Gaussian program package is different from the original one, that is, $0.5*E_X^{HF} + 0.5*E_X^{LSDA} + 0.5*\Delta E_X^{Becke88} + E_C^{LYP}$ (see also http://www.gaussian.com/g_ur/k_dft.htm).
(21) Handy, N. C.; Cohen, A. J. *Mol. Phys.* **2001**, *99*, 403–607.
(22) (a) Xu, X.; Goddard, W. A., III *Proc. Natl. Acad. Sci. U.S.A.* **2004**, *101*, 2673. (b) Xu, X.; Zhong, Q.; Muller, R. P.; Goddard, W. A., III *J. Chem. Phys.* **2005**, *122*, 014105. (c) Cerny, J.; Hobza, P. *Phys. Chem. Chem. Phys.* **2005**, *7*, 1624.
(23) Perdew, J. P.; Burke, K.; Ernzerhof, M. *Phys. Rev. Lett.* **1996**, *77*, 3865.
(24) Hamprecht, F. A.; Cohen, A. J.; Tozer, D. J.; Handy, N. C. *J. Chem. Phys.* **1998**, *109*, 6264.
(25) Lynch, B. J.; Fast, P. L.; Harris, M.; Trular, D. G. *J. Phys. Chem. A* **2000**, *104*, 4811.
(26) Kang, J. K.; Musgrave, C. B. *J. Chem. Phys.* **2001**, *115*, 11040.
(27) Quintal, M. M.; Karton, A.; Iron, M. A.; Boese, A. D.; Martin, J. M. L. *J. Phys. Chem. A* **2006**, *110*, 709.
(28) Boese, A. D.; Martin, J. M. L. *J. Chem. Phys.* **2004**, *121*, 3405.
(29) Stratmann, R. E.; Scuseria, G. E.; Frisch, M. J. *J. Chem. Phys.* **1998**, *109*, 8218.
(30) Wiberg, K. B.; Stratmann, R. E.; Frisch, M. J. *Chem. Phys. Lett.* **1998**, *297*, 60.
(31) Schirmer, J.; Dreuw, A. *Phys. Rev. A* **2007**, *75*, 022513.
(32) Dreuw, A.; Head-Gordon, M. *Chem. Rev.* **2005**, *105*, 4009.
(33) (a) Burke, K.; Werschnik, J.; Gross, E. K. U. *J. Chem. Phys.* **2005**, *123*, 062206. (b) Marques, M. A. L.; Gross, E. K. U. *Annu. Rev. Phys. Chem.* **2004**, *55*, 427.

(34) Elliott, P.; Burke, K.; Furche, F. **2007**, arXiv:cond-mat/0703590v1 [cond-mat.mtrl-sci].
(35) Runge, E.; Gross, E. K. U. *Phys. Rev. Lett.* **1984**, *52*, 997.
(36) Petersilka, M.; Gossmann, U. J.; Gross, E. K. U. *Phys. Rev. Lett.* **1996**, *76*, 1212.
(37) Casida, M. E. In *Recent Developments and Applications in Density Functional Theory*; Seminario, J. M., Ed.; Elsevier: Amsterdam, 1996.
(38) Casida, M. E. In *Recent Developments and Applications in Density Functional Methods, Part I*; Chong, D. P., Ed.; World Scientific: Singapore, 1995.
(39) Yanai, T.; Tew, D. P.; Handy, N. C. *Chem. Phys. Lett.* **2004**, *393*, 51.
(40) (a) Kobayashi, R.; Amos, R. D. *Chem. Phys. Lett.* **2006**, *420*, 106. (b) Kobayashi, R.; Amos, R. D. *Chem. Phys. Lett.* **2006**, *424*, 225. (c) Cai, Z.-L; Crossley, M. J.; Reimers, J. R.; Kobayashi, R.; Amos, R. D. *J. Phys. Chem. B* **2006**, *110*, 15624–15632.
(41) Zhao, Y.; Schultz, N. E.; Truhlar, D. G. *J. Chem. Theory Comput.* **2006**, *2*, 364.
(42) (a) Zhao, Y.; Truhlar, D. G *Org. Lett.* **2006**, *25*, 5753. (b) Zhao, Y.; Truhlar, D. G. *J. Chem. Theory Comput.* **2007**, *3*, 289. 3. Zhao, Y.; Truhlar, D. G. *Acc. Chem. Res.* **2008**, *41*, 157.
(43) Becke, A. D. *Phys. Rev. A* **1988**, *38*, 3098.
(44) Lee, C. T.; Yang, W. T.; Parr, R. G. *Phys. Rev. B* **1988**, *37*, 785.
(45) Perdew, J. P. *Phys. Rev. B* **1986**, *33*, 8832.
(46) Boese, A. D.; Handy, N. C. *J. Chem. Phys.* **2002**, *116*, 9559.
(47) Becke, A. D. *J. Chem. Phys.* **1996**, *104*, 1040.
(48) (a) Van Voorhis, T.; Scuseria, G. E. *J. Chem. Phys.* **1998**, *109*, 400. (b) Jaramillo, J.; Scuseria, G. E. *Chem. Phys. Lett.* **1999**, *312*, 269. (c) Johnson, E. R.; Wolkow, R. A.; DiLabio, G. A. *Chem. Phys. Lett.* **2004**, *394*, 334.
(49) Tao, J.; Perdew, J. P.; Staroverov, V. N.; Scuseria, G. E. *Phys. Rev. Lett.* **2003**, *91*, 146401.
(50) Zhao, Y.; Schultz, N. E.; Truhlar, D. G. *J. Chem. Phys.* **2005**, *123*, 161103.
(51) Adamo, C.; Barone, V. *J. Chem. Phys.* **1999**, *110*, 6158.
(52) Staroverov, V. N.; Scuseria, G. E.; Tao, J.; Perdew, J. P. *J. Chem. Phys.* **2003**, *119*, 12129.
(53) Heyd, J.; Scuseria, G. E.; Ernzerhof, M. *J. Chem. Phys.* **2003**, *118*, 8207.
(54) (a) Good, W. D. *J. Chem. Thermodyn.* **1972**, *4*, 709. (b) NIST. http://webbook.nist.gov/chemistry/.
(55) Thomas, L. L.; Christakis, T. J.; Jorgensen, W. L. *J. Phys. Chem. B* **2006**, *110*, 21198–21204.
(56) Jorgensen, W. L.; Maxwell, D. S.; Tirado-Rives, J. *J. Am. Chem. Soc.* **1996**, *118*, 11225–11236.
(57) Wiberg, K. B.; Wang, Y.-G.; Petersson, G. A.; Bailey, W. F. *J. Chem. Theory Comput.* **2009**, *5*, 1033.
(58) Alves, A. C. P.; Hollas, J. M. *Mol. Phys.* **1973**, *25*, 1305.
(59) Bracamonte, A. E.; Vaccaro, P. H. *J. Chem. Phys.* **2004**, *120*, 4638.
(60) (a) Burns, L. A.; Murdock, D.; Vaccaro, P. H. *J. Chem. Phys.* **2006**, *124*, 204307. (b) Burns, L. A.; Murdock, D.; Vaccaro, P. H. *J. Chem. Phys.* **2009**, *130*, 144304.
(61) Casadesus, R.; Vendrell, O.; Moreno, M.; Lluch, J. M. *Chem. Phys. Lett.* **2005**, *405*, 187.
(62) Zhao, Y.; Truhlar, D. G. *J. Phys. Chem. A* **2006**, *110*, 10478.
(63) Jorgensen, W. L.; Tirado-Rives, J. *J. Comput. Chem.* **2005**, *26*, 1689–1700.
(64) Frisch, M. J.; Trucks, G. W.; Schlegel, H. B.; Scuseria, G. E.; Robb, M. A.; Cheeseman, J. R.; Montgomery, J. A., Jr.; Vreven, T.; Kundin, K. N.; Burant, J. C.; Millam, J. M.; Iyengar, S. S.; Tomasi, J.; Barone, V.; Mennucci, B.; Cossi, M.; Scalmani, G.; Rega, N.; Petersson, G. A.; Nakatsuji, H.; Hada, M.; Ehara, M.; Toyota, K.; Fukuda, R.; Hasegawa, J.; Ishida, M.; Nakajima, T.; Honda, Y.; Kitao, O.; Nakai, H.; Klene, M.; Li, X.; Knox, J. E.; Hratchian, H. P.; Cross, J. B.; Adamo, C.; Jaramillo, J.; Gomperts, R; Stratmann, R. E.; Yazyev, O.; Austin, A. J.; Cammi, R.; Pomelli, C.; Ochterski, J. W.; Ayala, P. Y.; Morokuma, K.; Voth, G. A.; Salvador, P.; Dannenberg, J. J.; Zakrzewski, V. G.; Dapprich, S.; Daniels, A. D.; Strain, M. C.; Farkas, O.; Malick, D. K.; Rabuck, A. D.; Raghavachari, K.; Foresman, J. B.; Ortis J. V.; Cui, Q.; Baboul, A. G.; Clifford, S.; Cioslowski, J.; Stefanov, B. B.; Liu, G.; Liashenko, A.; Piskorz, P.; Komaromi, I.;. Martin, R. L.; Fox, D. J.; Keith, T.; Al-Laham, M. A.; Peng, C. Y.; Nanayakkara, A.; Challacombe, M.; Gill, P. M. W.; Johnson, B.; Chen, W.; Wong, M. W.; Gonzalez, C.; Pople, J. A., *Gaussian*, version E.05; Gaussian, Inc.: Wallingford, CT, 2006.
(65) Rablen, P. R.; Hadad, C. M. *CASGEN*; Yale University: New Haven, CT, 1993.

JP9077739